Published in final edited form as:
FEBS Lett. 2010 March 5; 584(5): 903–910. doi:10.1016/j.febslet.2009.12.058.

Identification of a novel splicing isoform of murine CGI-58

Xingyuan Yang[1,2], **Xin Lu**[1,2], and **Jun Liu**[1,2,*]

[1]Department of Pediatrics, University of Kentucky, Lexington, KY, USA

[2]Kentucky Pediatric Research Institute, University of Kentucky, Lexington, KY, USA

Abstract

The CGI-58 gene, mutations of which are linked to Chanarin-Dorfman syndrome, encodes a protein of the α/β hydrolase domain subfamily. We report here a new alternative splicing isoform of the murine CGI-58 gene, termed mCGI-58S. Sequence comparison indicates the lack of second and third exons in this cDNA variant. While the full length protein displayed perilipin-dependent localization to lipid droplets, mCGI-58S showed a predominant cytoplasmic staining when expressed in cells. mCGI-58S was incapable of activating ATGL but retained the capacity to acylate lysophosphatidic acid. Overexpression of mCGI-58S failed to promote lipid droplet turnover and loss of intracellular triacylglycerols. These results suggest that this splicing event may be involved in the regulation of lipid homeostasis.

Keywords

neutral lipid storage disease; lipolysis; triacylglycerol; lipid droplets; lysophosphatidic acid

1. Introduction

Chanarin-Dorfman syndrome (CDS) is a rare form of neutral lipid storage disease (NLSD) characterized by the accumulation of cytosolic lipid droplets containing triacylglycerol (TAG) in various tissues such as skin and liver as well as isolated cells including lymphocytes, macrophages and fibroblasts [1-4]. CDS is also termed NLSD with itchyosis (NLSDI) due to the fine white scaling phenotype associated with the impaired barrier function of the skin [3]. Earlier studies using fibroblasts obtained from CDS patients indicated a defect in the recycling of TAG-derived products such as mono- and diacylglycerols to glycerophospholipids [5,6]. A defect in the catabolism of TAG harboring long acyl chains was also shown in CDS fibroblasts [7]. In 2001, Lefevre *et al.* identified mutations of CGI-58 (Comparative Gene Identification 58; also known as α/β hydrolase fold–containing protein 5, ABHD5) as causative for CDS [8]. Separate studies demonstrated that in adipocytes CGI-58 was localized to lipid droplets via binding directly to perilipin [9,10]. However, the biochemical roles of CGI-58 in lipid metabolism and the mechanisms whereby mutations of CGI-58 lead to CDS remained unclear.

A major advance in understanding the function of CGI-58 was the discovery that the lipase activity of adipose triglyceride lipase (ATGL), the rate limiting enzyme for TAG catabolism,

*To whom correspondence should be addressed at: Department of Pediatrics, University of Kentucky, BBSRB B357, 741 South Limestone Street, Lexington, KY 40536-0509, Tel: (859) 257-4055, Fax: (859) 257-2120, jun.liu@uky.edu.

is highly dependent on the association with CGI-58 [11]. CGI-58 contains a canonical lipase motif, although the usual catalytic serine in GXSXG motif is replaced by asparagine. As a result, CGI-58 itself does not have a lipase activity. Upon interaction with CGI-58, ATGL TAG lipase activity increased up to 20-fold in cultured cells. Interestingly, CGI-58 mutants associated with CDS failed to activate ATGL [11], implicating that loss of ATGL activation may be involved in the pathogenesis of CDS. Overexpression of either ATGL or CGI-58 alone in COS-7 cells did not affect TAG storage, whereas overexpression of both proteins markedly reduced TAG deposition, indicating that the interaction between ATGL and CGI-58 is required for efficient lipolysis. In accordance with the role of CGI-58 in ATGL activation, silencing of CGI-58 expression was found to drastically reduce PKA-activated FA and glycerol release in both mouse 3T3-L1 [11] and human hMADs adipocytes [12].

Aside from its role in lipolysis, CGI-58 was recently identified as closely related to ICT1 [13], a yeast acyltransferase responsible for enhanced phospholipid synthesis [14]. Consistently, sequence analysis reveals that CGI-58 possess a C-terminal HX_4D motif common to proteins with acyltransferase activity. Like ICT1, CGI-58 was shown to be able to convert lysophophatidic acid (LPA) to phosphatidic acid (PA) in an acyl-CoA-dependent manner. Interestingly, overexpression of human CGI-58 in yeast showed an increase in the formation of PA along with an overall increase of total phospholipids [13]. Based upon these observations, it has been proposed that in coordination with its role in lipolytic activation, CGI-58 can promote recycling of TAG-hydrolyzed products into phospholipids, thereby maintaining the TAG balance in mammalian systems [13]. However, mutations of CGI-58 causal for CDS did not affect its activity as LPA acyltransferase [13], indicating that pathogenesis of CDS is not accounted for by the loss of such activity of CGI-58.

In the process of analyzing the expression of murine CGI-58, we found a shorter CGI-58 cDNA generated by alternative splicing. This splicing variant eliminates the second and the third exons, producing a protein unable to activate ATGL, but still able to function as a LPA acyltransferase. Thus, it could play a unique role in the regulation of TAG and phospholipid metabolism.

2. Materials and Methods

2.1 Cell culture

HeLa cells (ATCC) were cultured in DMEM containing 10% fetal bovine serum (FBS). Mouse 3T3-L1 preadipocytes were maintained in DMEM supplemented with 10% newborn calf serum, 100 U/mL penicillin G sodium, and 100 μg/mL streptomycin sulfate. Differentiation to adipocytes was induced by treatment of postconfluent cells with 10% FBS, 1 μg/mL insulin, 1 μM dexamethasone (DEX), and 0.5 mM isobutyl-1-methylzanthine (IBMX). The differentiation medium was withdrawn 3 days later and replaced with medium supplemented with 10% FBS and 1μg/mL insulin. After 2 days in insulin containing medium, the cells were then cultured in DMEM containing 10% FBS.

2.2 RNA extraction, PCR cloning of cDNA and construction of plasmids

Total RNA was prepared from mouse 3T3-L1 preadipocytes and adipocytes using the RNeasy Mini Kit (Qiagen) according to the manufacturer's instruction. cDNA was prepared from mRNA using SuperScript Reverse Transcriptase protocol (Invitrogen). RNA was extracted from mouse tissue was performed as described above. The sequences containing the complete open reading frame of mouse CGI-58 and shorter CGI-58 were amplified by PCR using ultra Pfu DNA Polymerase Mix (Stratagene). The primers designed to create restriction sites for subsequent cloning strategies are as follows: primer 1, CGI-58 forward (5′ - GCG GAT CCA

AAG CGA TGG CGG CGG AGG AGG- 3′); primer 2, CGI-58 reverse (5′ - CGC TCG AGT CAG TCT ACT GTG TGG CAG ATC - 3′).

The PCR products containing CGI-58FL and CGI-58S cDNA were cleaved by BamHI / XhoI. The digested products were purified and ligated in frame to BamHI (5′) and XhoI (3′) sites of the eukaryotic expression vector of pKMyc to generate constructs with a Myc epitope tag fused to the 5′ end of the cDNAs.

2.3 Transient transfection of HeLa cells and 3T3-L1 adipocytes

Transient transfection of HeLa cells was performed using Lipofectamine 2000 reagent according to the manufacturer's instructions. For immunofluorescence studies, 0.5 μg of each DNA construct was transfected into cells cultured on coverslips at low density in 6-well dishes. Cells were fixed 16-18 h post transfection. For immunoblotting analysis, 1.0 μg of each DNA was used in transfection of subconfluent cells cultured in 60-mm dishes. Cells were lysed 16-18 h post transfection. 3T3-L1 adipocytes were transfected by electroporation as described previously [15].

2.4 Cell lysis and immunoblotting

For immunoblotting, HeLa cells were washed twice with ice-cold PBS, and were lysed at 4° C with a buffer containing 50mM Tris-HCl (pH 8.0), 135mM NaCl, 10 mM NaF, 1% NP-40, 0.1% SDS, 0.5% sodium deoxycholate, 1.0 mM EDTA, 5% glycerol and protease inhibitors (1 tablet per 7 ml of buffer). The lysates were clarified by centrifugation at 10,000 × g for 10 min and then mixed with equal volume of 2× SDS sample buffer. The solubilized proteins were resolved by SDS-PAGE and transferred to nitrocellulose membranes. Individual proteins were blotted with primary antibodies against ATGL (Cell Signaling, 1:3,000) or Myc (Santa Cruz Biotech., 1:3,000) at appropriate dilutions. Peroxide-conjugated secondary antibodies were incubated with the membrane at a dilution of (1:5000). The signals were then visualized by enhance chemiluminescence (ECL Reagents, GE Healthcare).

2.5 Immunofluorescence staining and confocal microscopy

HeLa cells and adipocytes were maintained at proper densities on glass coverslips placed in 6-well dishes. Following the fixation with 3% paraformaldehyde in PBS for 30 min and permeabilization with 0.5% Triton X-100 in PBS for 5 min, cells were quenched with 100 mM glycine in PBS for 20 min and then blocked with 1% BSA in PBS for 1h. The cells were then exposed to Myc and/or perilipin (Abcam) antibodies (1:1,000) for 2 h at room temperature. Following three washes with PBS, the cells were treated for 1 h in blocking solution with Alexa Fluor secondary antibodies diluted to 2 μg/μl. Samples were mounted on glass slides with Vectashield mounting medium with DAPI and examined under a Leica SP5 inverted confocal microscope.

2.6 In vitro transcription-and-translation expression and TAG hydrolase activity assay

In vitro transcription/translation was carried out by using TNT® SP6 High-Yield Protein Expression System according to the manufacture's instruction. Specifically, 10 μg vector DNA per reaction was used to produce ATGL, CGI-58L and CGI-58S for TAG hydrolase assays. The TAG hydrolase activity against ^{3}H-labled triolein was measured as described previously [11,16]. A total of 35μl of reaction mixture were pre-diluted with 65μl of cell extraction buffer. The resulting 0.1ml of reaction mixture was then combined with 0.1ml of substrate solution in the TAG hydrolase activity measurement.

2.7 LPA acyltransferase assay

This assay was performed as described previously [13,14]. Briefly, the reaction mixture contained 50μM 1- oleoyl-[oleoyl-9,10-^{3}H] LPA (220,000dpm/assay) and 20mM acyl-CoA in lysis buffer containing of Tris-HCL (pH 8.0) and 300mM NaCl with a total volume of 100μl. The reaction was carried out at 30°C for 10min. The lipids were separated on a TLC plate using chloroform: methanol: acetone: acetic: water (50:10:20:15.5, v/v/v/v) as the solvent system. The TLC plates were air dried and subjected to autoradiography.

2.8 Measurement of intracellular TAG content

TAG accumulation was measured using a triglyceride assay kit (Zenbio). Briefly, HeLa cells plated in 24-well dishes were washed and lysed in provided lysis buffer. The triglyceride assay reagents were added according to the manufacturer's instructions. The optical density of the mixture was measured at 540 nm using a spectrophotometer plate reader.

3. Results

3.1 Alternatively spliced variant of murine CGI-58 gene

During the analysis of CGI-58 expression by RT-PCR, we detected two distinct CGI-58 transcripts in murine 3T3-L1 preadipocytes and adipocytes, the expected CGI-58 full length messenger and a shorter fragment not described previously (Fig, 1A). A separate RT-PCR amplification confirmed the existence of the same variants in mouse tissues such as liver, pancreas and fat, though the ratio of expression between the two appears to vary depending on the specific tissue type (Fig. 1B). Since PCR reactions were carried out using specific primers complementary to sequences containing the 5′ translation start site and the 3′ stop codon of murine CGI58 cDNA (primers 1 and 2, see Section 2), we thought that a process of alternative splicing could account for the generation of this novel fragment. To check this hypothesis, both PCR products were sequenced. While the major PCR fragment of 1053 bp is identical with the published CGI-58 cDNA, the minor fragment of 594 bp lacks an internal sequence of 495 bp within the 5′ region of the full-length sequence (GeneBank accession number NM_026179). This structure strongly suggests that this shortened cDNA molecule represents a new spliced variant of murine CGI-58. Alignment analysis using BLAST program (NCBI) with mouse genomic and cDNA sequences of CGI-58 indicates that flanking nucleotides of divergence point among sequences of this 594 bp fragment perfectly match with exonic sequences from exon1/intron1 and intron3/exon4 junctions, conforming that entire exon 2 and exon 3 are spliced out in the shorter fragment (Fig. 1C). This result shows that a splicing event is involved in the generation of this CGI58 variant that includes the first ATG-containing exon followed by exons 4-7. We have named this novel mouse CGI-58 isoform mCGI-58S as opposed to the full length version which we refer to as mCGI-58FL.

The mCGI-58FL is a 351-amino acid protein. Like its human orthologue, mCGI-58FL belongs to α/β hydrolase family. The α/β hydrolase fold is localized between amino acids 104 and 345 of mCGI-58FL. The protein contains a “pseudo-catalytic triad” at positions 153(Asn)/327 (His)/301(Asp), with the nucleophilic serine usually found in the typical GXSXG motif being replaced by an asparagine (Asn-153) [8]. Moreover, the full-length protein contains a putative lipid binding domain between amino acids 72 and 90 that is highly hydrophobic, and a HX_4D motif between amino acids 335 and 340 that is present in proteins with acyltransferase activity [13,17]. As shown Fig. 1D, the predicted open reading frame of CGI-58S encodes for a 202-amino acid protein that lacks the lipid binding domain and the GXNXG motif. However, the HX_4D motif for acyltransferase activity is retained in mCGI-58S, suggesting that this splicing variant may still function as a LPA acyltransferase as the full-length protein.

3.2 Lipid droplet localization of mCGI-58FL vs. mCGI-58S

In an attempt to identify the functional differences between mCGI-58S and its full length counterpart, we decided to examine their lipid droplet localization in nonadipocyte cells and adipocytes. Both proteins were tagged with a Myc epitope tag at the N-terminus, and immunoblotting analysis confirmed the size of the proteins when expressed in HeLa cells (Fig. 1E). After a prolonged treatment with oleic acid to enhance lipid droplet formation, cells were fixed and subjected to immunofluorescence staining with specific anti-Myc antibodies. Lipid droplets were co-stained with a BODIPY nonpolar fluorescence dye that is selective for neutral lipids including TAG. As shown in Fig. 2A upper panel, Myc-mCGI-58FL alone displayed a diffusive distribution throughout the cytoplasm, with a very low level of staining at the surface of lipid droplets. Coexpression of perilipin promoted the lipid droplet localization of mCGI-58L (Fig. 2B, upper panel), consistent with the conclusion derived from previous studies that interaction with perilipin plays a critical role in recruiting CGI-58 to lipid droplets [9, 10]. In comparison, Myc-mCGI-58S alone exhibited a punctuate pattern of localization that did not overlap with lipid droplets (Fig. 2A, lower panel). Interestingly, coexpression of perilipin conferred no effect on this localization of mCGI-58S (Fig. 2B, lower panel). Similar results were obtained from overexpression studies using 3T3-L1 adipocytes. As shown in Fig. 2C, ectopic mCGI-58S failed to localize to lipid droplets, whereas the full length protein showed a clear presence at the surface of lipid droplets along with a punctuate distribution in the cytoplasm. Taken together, these results suggest that the region encoded by exons 2 and 3 and missing in mCGI-58S is required for the perilipin-dependent localization to lipid droplets.

3.3 CGI-58S is not a coactivator of ATGL lipase activity

The TAG lipase activity of ATGL is largely dependent on the presence of CGI-58 [11,18]. To test whether mCGI-58S would also work as a coactivator of ATGL, we assayed the enzyme activity of ATGL using a cell free system in the presence of either mCGI-58FL or mCGI-58S. Myc-CGI-58FL, Myc-CGI-58S and ATGL were prepared separately by an *in vitro* transcription/translation method employing wheat germ extracts. These proteins were efficiently produced at comparable levels as revealed by anti-Myc immunoblotting of the resultant extracts (Fig. 3A). In the subsequent enzymatic assays using triolein as substrate, the addition of CGI-58FL-containing extracts to ATGL-containing extracts resulted in an over 7-fold increase in the lipase activity when compared to ATGL extracts alone (Fig. 3B). By contrast, CGI-58S was incapable of significantly activating ATGL when their respective extracts were combined. To assess if the presence of mCGI-58S would influence the ability of the full length protein to activate ATGL, the extracts containing all three proteins were mixed prior to the initiation of the lipase enzyme reaction. As shown in Fig. 3B, mCGI-58FL activated ATGL to the same degree in the presence as compared to in the absence of mCGI-58S, indicating that the shorter variant does not interfere with the full length protein in the augmentation of ATGL activity.

3.4 CGI-58S retains LPA acyltransferase activity

Previous work by Gosh *et al.* has shown that CGI-58 exhibits acyl-CoA-dependent acyltransferase activity for LPA, leading to the generation of PA [13]. Since mCGI-58S retains the HX_4D motif, we asked whether mCGI-58S would still function as a LPA acyltransferase as the full-length protein. In this regard, Myc-CGI-58FL and Myc-CGI-58S proteins were prepared by the *in vitro* transcription/translation, and their LPA acyltransferase activity was measured in the resultant extracts by using the established method [13]. As shown in Fig. 3C, the two proteins were equally effective in mediating the formation of PA via the incorporation of oleoyl-CoA into LPA. Thus, the shorter variant of mCGI-58 indeed possesses LPA acyltransferase activity.

3.5 Effects of CGI-58S on TAG content and lipid droplet degradation

The impact of mCGI-58FL vs. mCGI-58S on intracellular TAG content was assessed by comparing the cellular TAG levels and the lipid droplet morphology in HeLa cells. Cells were transfected with vector alone, mCGI-58FL or mCGI-58S with comparable efficiencies as revealed by anti-Myc immunostaining and counter staining of nuclei with DAPI dye. For the measurement of intracellular TAG content, transfected cells were first treated with oleic acid to promote TAG accumulation. In comparison to transfection with vector alone, mCGI-58FL slightly decreased while mCGI-58S slightly increased intracellular TAG content (Fig. 4A). Interestingly, in response to nutrient withdrawal following the oleic acid treatment, cells expressing mCGI-58FL exhibited a more drastic loss of intracellular TAG than those transfected with vector alone. On the other hand, expression of mCGI-58S did not promote such loss of TAG induced by the nutrient withdrawal. For studies of lipid droplets degradation, untransfected cells were mixed with cells either expressing mCGI-58FL or mCGI-58S. As shown in Fig. 4B, overloading cells with oleic acid resulted in accumulation of large lipid droplets in both transfected cells and neighboring untransfected cells. No obvious difference in size and number of lipid droplets were observed in untransfected cells and cells expressing either mCGI-58FL or mCGI-58S. However, upon nutrient withdrawal, lipid droplets in cells expressing mCGI-58-FL underwent more pronounced degradation than those in untransfected cells. In comparison, expression of mCGI-58S did not enhance the turnover of lipid droplets. Collectively, these results suggest that the shorter variant of CGI-58 does not share the function of the full length protein in the regulation of TAG catabolism.

4. Discussion

In humans, mutations of CGI-58/ABHD5 are associated with CDS, characterized by excessive accumulation of TAG in multiple tissues and ichthyosis [1-4]. Sequence comparison of human CGI-58 and the murine orthologue reveals 94% identity and 96% homology, implying that they are functionally interchangeable. In this study, we describe that alternative splicing generates a novel shorter cDNA variant molecule of murine CGI-58, which we have named CGI-58S. Like the full length isoform, CGI-58S is expressed in cultured 3T3-L1 adipocytes as well as in tissues such as fat, liver and pancreas, suggesting that it could be functionally relevant in various settings. Previously Northern analyses of CGI-58 in mouse tissues have revealed two mRNA specifies of ~1.4 and 3.2 kb, which presumably vary in the length of their 3′ untranslated regions [10,11]. It is possible that the mRNA of CGI-58S, which was detected by RT-PCR amplification, has not been identified earlier by Northern analysis due to its low expression level relative to the full length mRNA.

The biochemical functions of CGI-58 protein had been largely unclear until the discovery of CGI-58 as a potent co-activator of ATGL [11]. Interestingly, mCGI-58S, lacking a sequence of 143 amino acids encoded by exons 2 and 3, does not share this role of the full length protein in lipolysis. In HeLa cells, overexpression CGI-58S did not promote either turnover of lipid droplet or decrease in intracellular TAG as compared to CGI-58FL. Moreover, in a standard TAG lipase assay against triolein substrate, CGI-58S exhibited no activating effect on ATGL, while CGI-58FL was able to enhance ATGL activity by 7-8 folds. Furthermore, it is unlikely that CGI-58S would directly influence CGI-58FL in the regulation of lipolysis. This notion is supported by the observations that CGI-58S is incapable of localizing onto lipid droplets, and the presence of CGI-58S did not affect the activation of ATGL by CGI-58FL *in vitro*. Although the mechanisms by which the full-length CGI-58 regulates ATGL remains elusive, we speculate that the absence of three structural features in mCGI-58S, namely the putative lipid binding motif, the GXNXG “pseudo esterase/lipase” motif and Gln130, may explain its inability to activate ATGL. While the functional contribution of the lipid binding sequence and the GXNXG motif remain uncharacterized, the Gln130 is known to be important for the

interaction with ATGL [9]. The Q130P mutation, causal for CDS, was shown previously to completely eliminate the ATGL-activating capacity of the full length CGI-58 [11].

CGI-58 was previously shown to localize to lipid droplets via its interaction with perilipin in adipocytes and with ADRP/adipophilin in nonadipocyte cells [9,10]. In a recently proposed model of adipocyte lipolysis [4,19], CGI-58 binds to perilipin on the surface of lipid droplets and is unable to activate ATGL in the basal state. Upon β-adrenergic stimulation, CGI-58 dissociates from phosphorylated perilipin and complexes with ATGL, thereby activating lipolysis. In our hands, CGI-58S displayed a different subcellular distribution from CGI-58FL when overexpressed in cultured cells. In 3T3-L1 adipocytes that express a high level of endogenous perilipin, CGI-58FL was expectedly localized on the surface of lipid droplets, whereas CGI-58S resided predominantly in the cytoplasm. Notably, CGI-58FL also displayed a punctuate localization in the cytoplasm in addition to lipid droplets. Since ATGL resides in an ER-related membrane compartment when not localized to lipid droplets [20], we speculate that CGI-58FL may occur in association with similar membrane structures. The specific involvement of perilipin in the lipid droplet localization of CGI-58 was later evaluated by a reconstitution experiment using HeLa cells that express no endogenous perilipin. When expressed alone in HeLa cells, neither CGI-58FL nor CGI-58S showed noticeable localization to lipid droplets. Similar to what was observed in 3T3-L1 preadipocytes [10], adipophilin at the endogenous level apparently failed to efficiently recruit CGI-58FL to the lipid droplets in HeLa cells. Interestingly, the addition of perilipin in HeLa cells via coexpression resulted in a profound recruitment of CGI-58FL to the lipid droplets. However, the ectopic perilipin had no effect on the localization of CGI-58S. The findings are in accordance with the notion that nearly the entire region of CGI-58 is required for the co-localization with perilipin on the surface of lipid droplets. Since CGI-58S lacks the putative lipid-binding motif, it remains to be determined whether the loss of lipid droplet localization of CGI-58S is due to its inability to bind perilipin or to interact directly with lipids or both.

CGI-58 was recently demonstrated to exhibit activity as an acyl-CoA-dependent LPA acyltransferase [13]. Although the *in vivo* relevance of this finding is still unknown, the acyltransferase activity of CGI-58 is postulated to facilitate recycling of products derived from TAG hydrolysis into glycerophospholipids [13]. Thus, CGI-58 may function in both lipolysis and synthesis of phospholipids, depending on its subcellular localization. Our data demonstrated that mCGI58S, with an intact HX_4D motif, possessed a similar LPA acyltransferase activity as the full-length protein. Since it is predominantly localized in the cytoplasm, CGI-58S probably mainly function as a LPA acyltransferase in the production of PA. PA is common precursor for both TAG and glycerophopholipids, and its final fate may be decided by the lipolytic status in the cells. In this regard, it is tempting to speculate that LPA acylation mediated by CGI-58S and TAG hydrolysis driven by CGI-58FL may work coordinately to facilitate net flux of PA to phospholipids.

In summary, the present study highlights the existence of a novel splicing variant of CGI-58 in mouse. This splicing event may potentially be involved in the regulation of intracellular lipid homeostasis. Thus, it would be interesting to determine if such splicing is subject to regulation by specific hormonal and/or nutritional conditions. Moreover, no equivalent alternative spliced isoform to mCGI-58S has been described in other species including human. It is possible that in other mammals, alternative mechanisms would account for generating a functional counterpart of mCGI-58S. Furthermore, our findings provide valuable information to functional studies of CGI-58, most of which have employed mouse cell lines such as 3T3-L1 adipocytes and genetically modified mice.

Acknowledgments

The work was supported by a NIH grant DK 078742 and a Center of Biomedical Research Excellence pilot grant from the University of Kentucky (5P20 RR0202171) to J.L.

References

1. Dorfman ML, Hershko C, Eisenberg S, Sagher F. Ichthyosiform dermatosis with systemic lipidosis. Arch Dermatol 1974;110:261–6. [PubMed: 4277517]
2. Chanarin I, Patel A, Slavin G, Wills EJ, Andrews TM, Stewart G. Neutral-lipid storage disease: a new disorder of lipid metabolism. Br Med J 1975;1:553–5. [PubMed: 1139147]
3. Schweiger M, Lass A, Zimmermann R, Eichmann TO, Zechner R. Neutral lipid storage disease: genetic disorders caused by mutations in adipose triglyceride lipase/PNPLA2 or CGI-58/ABHD5. Am J Physiol Endocrinol Metab 2009;297:E289–96. [PubMed: 19401457]
4. Yamaguchi T, Osumi T. Chanarin-Dorfman syndrome: deficiency in CGI-58, a lipid droplet-bound coactivator of lipase. Biochim Biophys Acta 2009;1791:519–23. [PubMed: 19061969]
5. Igal RA, Coleman RA. Neutral lipid storage disease: a genetic disorder with abnormalities in the regulation of phospholipid metabolism. J Lipid Res 1998;39:31–43. [PubMed: 9469583]
6. Igal RA, Coleman RA. Acylglycerol recycling from triacylglycerol to phospholipid, not lipase activity, is defective in neutral lipid storage disease fibroblasts. J Biol Chem 1996;271:16644–51. [PubMed: 8663220]
7. Hilaire N, Salvayre R, Thiers JC, Bonnafe MJ, Negre-Salvayre A. The turnover of cytoplasmic triacylglycerols in human fibroblasts involves two separate acyl chain length-dependent degradation pathways. J Biol Chem 1995;270:27027–34. [PubMed: 7592952]
8. Lefevre C, et al. Mutations in CGI-58, the gene encoding a new protein of the esterase/lipase/thioesterase subfamily, in Chanarin-Dorfman syndrome. Am J Hum Genet 2001;69:1002–12. [PubMed: 11590543]
9. Yamaguchi T, Omatsu N, Matsushita S, Osumi T. CGI-58 interacts with perilipin and is localized to lipid droplets. Possible involvement of CGI-58 mislocalization in Chanarin-Dorfman syndrome. J Biol Chem 2004;279:30490–7. [PubMed: 15136565]
10. Subramanian V, et al. Perilipin A mediates the reversible binding of CGI-58 to lipid droplets in 3T3-L1 adipocytes. J Biol Chem 2004;279:42062–71. [PubMed: 15292255]
11. Lass A, et al. Adipose triglyceride lipase-mediated lipolysis of cellular fat stores is activated by CGI-58 and defective in Chanarin-Dorfman Syndrome. Cell Metab 2006;3:309–19. [PubMed: 16679289]
12. Bezaire V, et al. Contribution of Adipose Triglyceride Lipase and Hormone-sensitive Lipase to Lipolysis in Human hMADS Adipocytes. J Biol Chem. 2009
13. Ghosh AK, Ramakrishnan G, Chandramohan C, Rajasekharan R. CGI-58, the causative gene for Chanarin-Dorfman syndrome, mediates acylation of lysophosphatidic acid. J Biol Chem 2008;283:24525–33. [PubMed: 18606822]
14. Ghosh AK, Ramakrishnan G, Rajasekharan R. YLR099C (ICT1) encodes a soluble Acyl-CoA-dependent lysophosphatidic acid acyltransferase responsible for enhanced phospholipid synthesis on organic solvent stress in Saccharomyces cerevisiae. J Biol Chem 2008;283:9768–75. [PubMed: 18252723]
15. Yamauchi K, Pessin JE. Insulin receptor substrate-1 (IRS1) and Shc compete for a limited pool of Grb2 in mediating insulin downstream signaling. J Biol Chem 1994;269:31107–14. [PubMed: 7983051]
16. Zimmermann R, et al. Fat mobilization in adipose tissue is promoted by adipose triglyceride lipase. Science 2004;306:1383–6. [PubMed: 15550674]
17. Heath RJ, Rock CO. A conserved histidine is essential for glycerolipid acyltransferase catalysis. J Bacteriol 1998;180:1425–30. [PubMed: 9515909]
18. Schweiger M, et al. The C-terminal region of human adipose triglyceride lipase affects enzyme activity and lipid droplet binding. J Biol Chem 2008;283:17211–20. [PubMed: 18445597]

19. Zechner R, Kienesberger PC, Haemmerle G, Zimmermann R, Lass A. Adipose triglyceride lipase and the lipolytic catabolism of cellular fat stores. J Lipid Res 2009;50:3–21. [PubMed: 18952573]
20. Soni KG, Mardones GA, Sougrat R, Smirnova E, Jackson CL, Bonifacino JS. Coatomer-dependent protein delivery to lipid droplets. J Cell Sci 2009;122:1834–41. [PubMed: 19461073]

List of abbreviations

CGI-58	comparative gene identification-58
CDS	Chanarin-Dorfman Syndrome
LPA	lysophosphatidic acid
PA	phosphatidic acid
ATGL	adipose triglyceride lipase
TAG	triacylglycerol

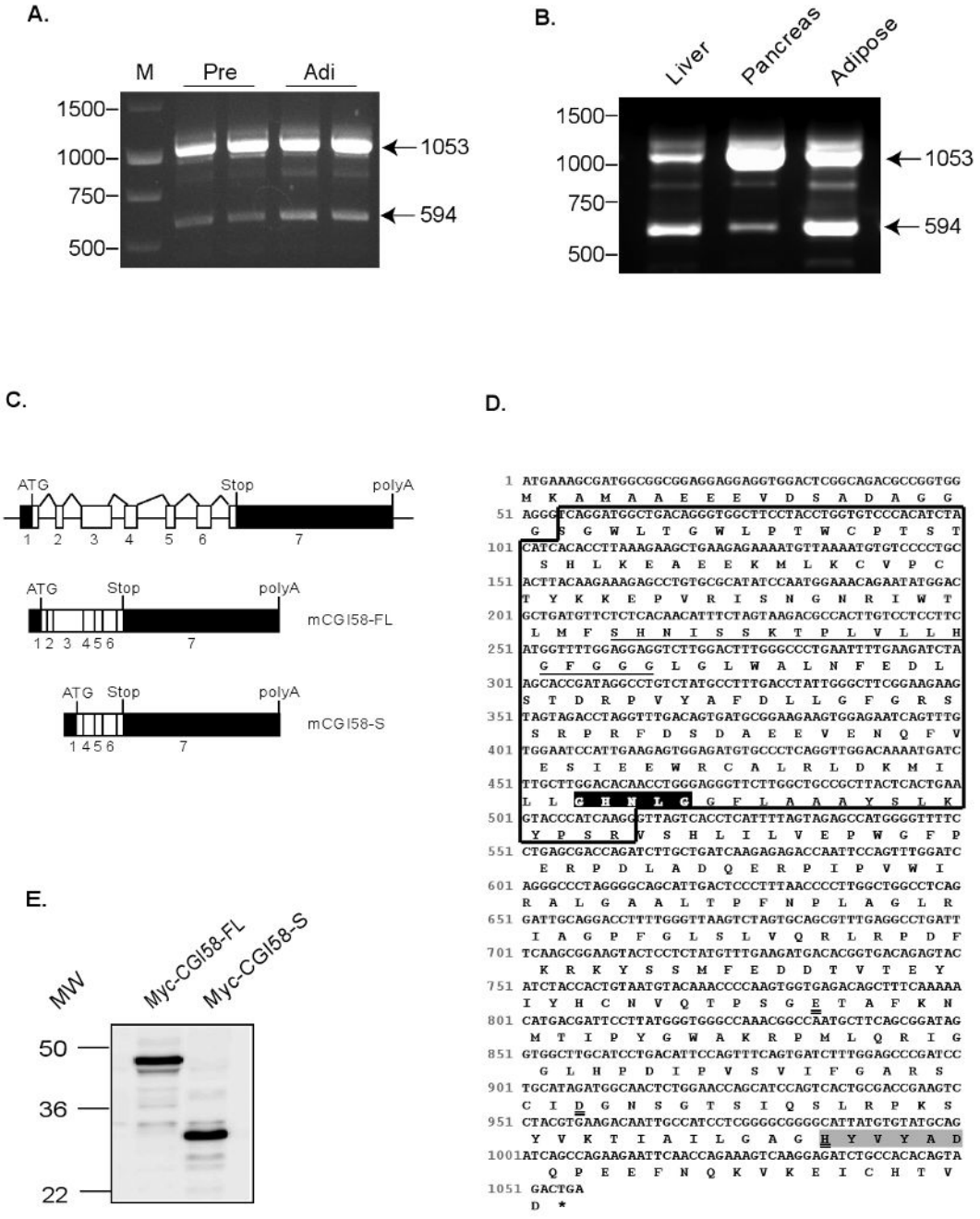

Figure 1. Identification of a new alternatively spliced murine CGI58

(A) RT-PCR amplification of murine mRNAs from preadipoctes and adipocytes. **(B)** RT-PCR analysis of mouse adipose, liver and pancreas RNA. RT was performed with random priming and equivalent aliquots of cDNA were used for PCR amplification. The 1053 bp cDNA corresponds to the full length murine CGI-58(GeneBank accession number NM_026179); the 594bp cDNA was identified as a novel spliced CGI-58 variant. **(C)** A schematic picture of murine CGI-58 genomic structure and its putatived transcripts. Black boxes represents the 5′ and 3′ untranslated regions. **(D)** Murine CGI-58S cDNA sequence with coding sequences capitalized. Square Box shows the alternative spliced region encoded by exon 2 and exon 3. Underlined sequence is a putative lipid binding domain. The conserved GXNXG motif and

HX_4D motif are indicated in bold in black and grey areas, respectively. Histidine (H329) and the putative third residue of the catalytic triad, either glutamate (E262) or aspartate (D303) are indicated by double underlines. **(E)** Transient expression of proteins in HeLa cells was analyzed by immunoblotting with anti-Myc antibody.

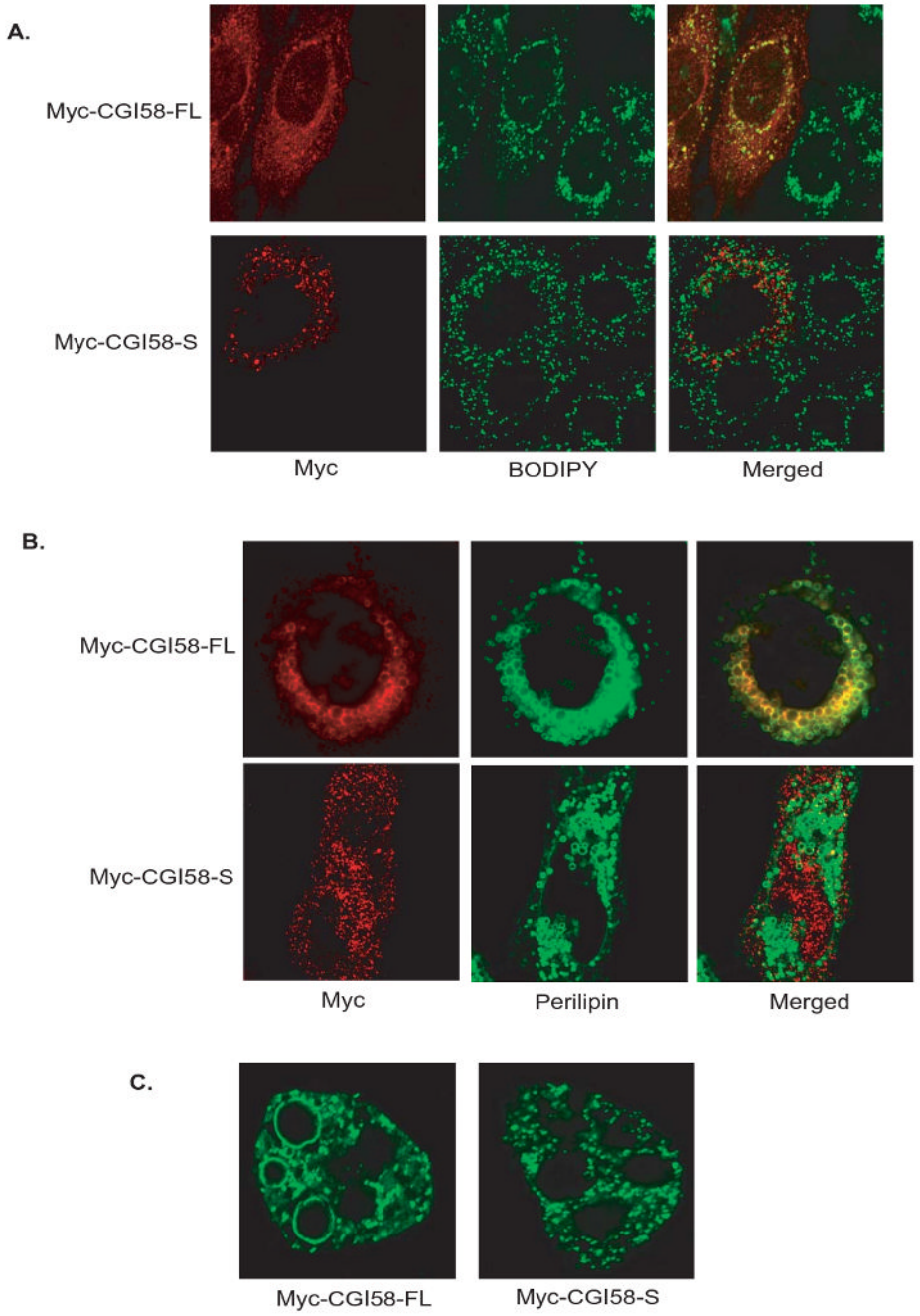

Figure 2. Lipid droplet localization of murine GGI-58 isoforms

(A) HeLa cells transfected with Myc-CGI-58L or Myc-CGI-58S were incubated under normal growth conditions with 400 μM of oleic acid complexed to albumin for 3 h. Immunofluorescence staining with anti-Myc antibody (red) was performed to reveal the respective proteins, Myc-CGI-58L (upper panel) or Myc-CGI-58S (lower panel). Lipid droplets were co-stained with BODIPY 493/503 fluorescence dye (green). **(B)** Perilipin was coexpressed with either Myc-CGI-58L or Myc-CGI-58S in HeLa cells. Cells were treated with oleic acid as in **(A)**, and co-stained with Myc (red) and perilipin (green) antibodies. (**C)** Overexpression of CGI-58L or CGI-58S in adipocytes was achieved via electroporation. Immunofluorescence staining with Myc antibody (green) was analyzed 3 days later.

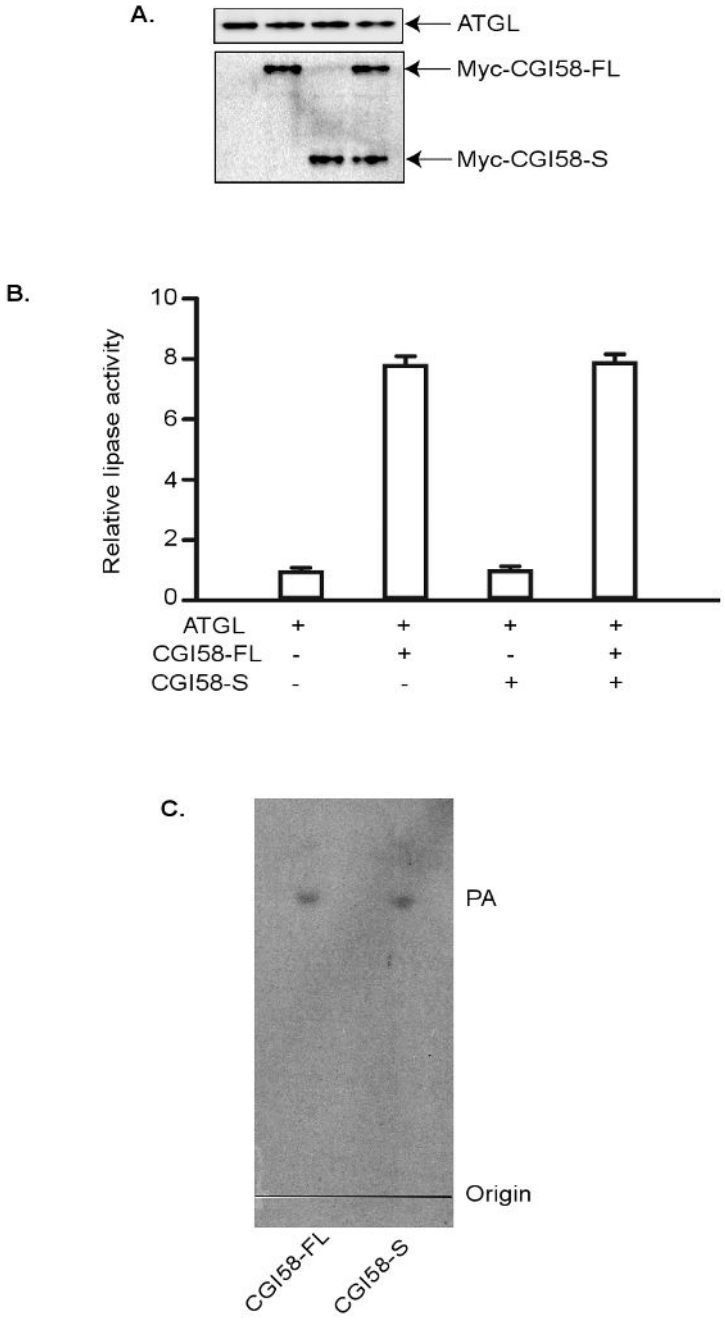

Figure 3. Effects of CGI-58 isoforms on TAG hydrolase activity or LPA acyltransferase activity

ATGL, mCGI-58L and mCGI-58S produced by using *in vitro* translation system. **(A) & (B)** Protein were mixed and then subjected to immunoblotting analysis with ATGL and Myc antibodies **(A)** and TAG hydrolase activity assays **(B)**. The TAG hydrolase activity in the cell lysate was measured using ^{3}H-labeled triolein as substrate. The activity was expressed as fold difference compared to activity in extracts containing ATGL-alone. Data are shown as mean ± SD and represent three independent experiments. **(C)** LPA acyltransferase activity was monitored under the standard assay conditions with equivalent amounts of proteins.

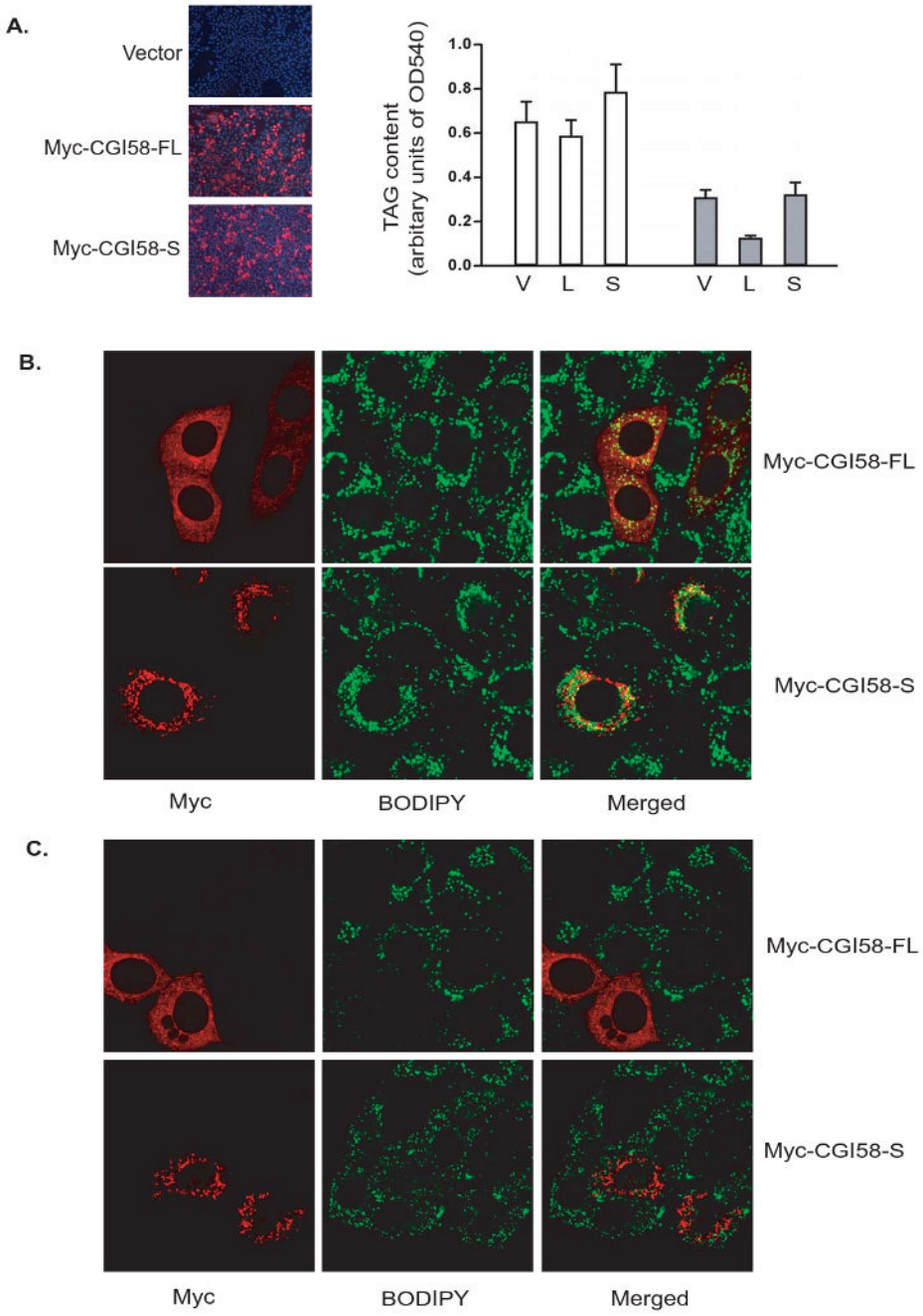

Figure 4. Effects of GGI-58 isoforms on intracellular TAG content and lipid droplet degradation

(A) *Left panel:* HeLa cells were transfected with vector alone (V), Myc-CGI-58FL (L) or Myc-CGI-58S (S). Immunofluorescence staining with anti-Myc antibody (red) was performed to reveal the transfected cells. Nuclei were co-stained with DAPI fluorescence dye (blue). *Right panel:* Following transfection, cells were incubated under normal growth conditions with 400 μM of oleic acid complexed to albumin for 24 h (white bars). A separate set of cells were incubated in serum- and glucose-free medium for 4h following 24h of incubation with 400 μM of oleic acid complexed to albumin (grey bars). The TAG content was determined as described in *Materials and Methods*. Data are shown as mean ± SD and represent three independent experiments. **(B)** HeLa cells transfected with Myc-CGI-58FL or Myc-CGI-58S

were mixed with untransfected cells followed by treatment with oleic acid for 24h. Immunofluorescence staining with Myc antibody (red) was performed, and lipid droplets were co-stained with BODIPY 493/503 fluorescence dye (green). **(C)** Same experiments as in **(B)** except that cells were incubated in serum- and glucose-free medium for 4h following 24h of oleic acid treatment.